

Probing Interaction-Induced Ferromagnetism in Optical Superlattices

J. von Stecher,¹ E. Demler,^{2,3} M. D. Lukin,^{2,3} and A. M. Rey¹

¹JILA, University of Colorado and National Institute of Standards and Technology, Boulder, Colorado 80309-0440,

²Physics Department, Harvard University, Cambridge, Massachusetts, 20138,

³Institute for Theoretical Atomic, Molecular and Optical Physics, Cambridge, Massachusetts 02138, USA

Abstract. We propose a method for controllable preparation and detection of interaction-induced ferromagnetism in ultracold fermionic atoms loaded in optical superlattices. First, we discuss how to probe and control Nagaoka ferromagnetism in an array of isolated plaquettes (four lattice sites arranged in a square). Next, we allow for weak interplaquette tunneling. Since ferromagnetism is unstable in the presence of weak interplaquette couplings, we propose to mediate long-range ferromagnetic correlations via double-exchange processes by exciting atoms to the first vibrational band. We calculate the phase diagram of the two-band plaquette array and discuss conditions for the stability and robustness of the ferromagnetic phases in this system. Experimental implementations of the proposed schemes are discussed.

1. Introduction

The origin of ferromagnetism in itinerant electron systems remains an important open problem in condensed matter physics. Mean field approaches, such as the Hartree-Fock approximation [1] and the Stoner criterion [2] for ferromagnetic instabilities, are extremely unreliable since they overestimate the stability of the magnetic-ordered phases [3]. The only rigorous example of ferromagnetism in the generic Hubbard model [4], predicted by Nagaoka in 1965 [5], was proven for a system with one fewer electron than half filling (i.e., one hole) in the limit of infinite interactions. Even though such a ferromagnetic state is an iconic example of a strongly correlated many-body state, it is highly unstable and counter examples indicating the absence of ferromagnetism with two or more holes have been found [6].

The experimental observation of Nagaoka ferromagnetism (NF) is a challenging task, as it requires a system with a finite and controllable number of holes. Even though there have been recent attempts to explore Nagaoka ferromagnetism using arrays of quantum dots [7], the exponential sensitivity of the tunneling rates to the interdot distance and the random magnetic field fluctuations induced by the nuclear spin background have prevented its direct experimental observation.

Here, we propose to use cold fermionic atoms in optical superlattices for the controllable observation of interaction-induced ferromagnetism. First, we show how to probe the onset of NF in an array of isolated plaquettes (four lattice sites in a square geometry). Next, we discuss how to engineer long-range ferromagnetic correlations, starting from the isolated plaquette arrays. Since weak coupling of the plaquettes destroys ferromagnetism [8], we instead propose to use additional atoms loaded in excited bands. The underlying idea is to use Hund's rule couplings [9] to favor local ferromagnetic alignment among the atoms in different bands and a double-exchange mechanism (tunneling-induced alignment of the spins) [10] to stabilize ferromagnetic correlations between adjacent plaquettes. Exact numerical calculations for an array of weakly coupled plaquettes confirm the existence of stable ferromagnetic order in this two-band setup. Finally, we discuss methods for experimental preparation and detection of the ferromagnetic correlations.

2. Probing Nagaoka ferromagnetism in superlattices.

The low-energy physics of fermionic atoms loaded in the lowest vibrational band of an optical lattice is well described by the Hubbard Hamiltonian:

$$\hat{H} = - \sum_{\langle r, r' \rangle, \sigma} J_{r, r'} \hat{c}_{r\sigma}^\dagger \hat{c}_{r'\sigma} + U \sum_r \hat{n}_{\uparrow r} \hat{n}_{\downarrow, r}, \quad (1)$$

where $J_{r, r'} = J$ is the tunneling energy, and U is the onsite interaction energy. In Eq. (1), $\hat{c}_{r\sigma}$ are fermionic annihilation operators, $\hat{n}_{r\sigma} = \hat{c}_{r\sigma}^\dagger \hat{c}_{r\sigma}$ are number operators, $r = 1, \dots, L$ labels the lattice sites, and $\langle r, r' \rangle$ in the summation indicates that the sum is restricted to nearest neighbors.

Before starting let us explicitly state Nagaoka theorem [5]: “Let the tunneling matrix element between lattice sites r and r' be negative, $J_{rr'} < 0$, for any $r \neq r'$ and $U = \infty$ and let the number of fermions be $N = L - 1$, with L the total number of sites. If the lattice satisfies certain connectivity condition, then the ground state has total spin $S = N/2$ and it is unique, apart from a trivial $(N + 1)$ -fold spin degeneracy”.

The notion of “connectivity” requires that each site in the lattice is contained in a loop (of non-vanishing $J_{rr'}$) and furthermore that the loops should pass through no more than four sites [11]. The requirement $J_{rr'} < 0$ is just the opposite of that assumed in most discussions of the Hubbard model. However, in bipartite lattices, there is always a canonical transformation connecting $J_{rr'} < 0$ and $J_{rr'} > 0$.

From the conditions of the theorem it is clear that the minimal geometry to observe Nagaoka ferromagnetism is a triangle, however a triangle is a trivial example since in this case either the ground state is always a singlet (case $J_{r,r'} = J > 0$) or it is always a triplet ($J < 0$) \ddagger . The first non trivial example of Nagaoka crossing takes place in a plaquette loaded with three fermions(Fig. 1(a)).

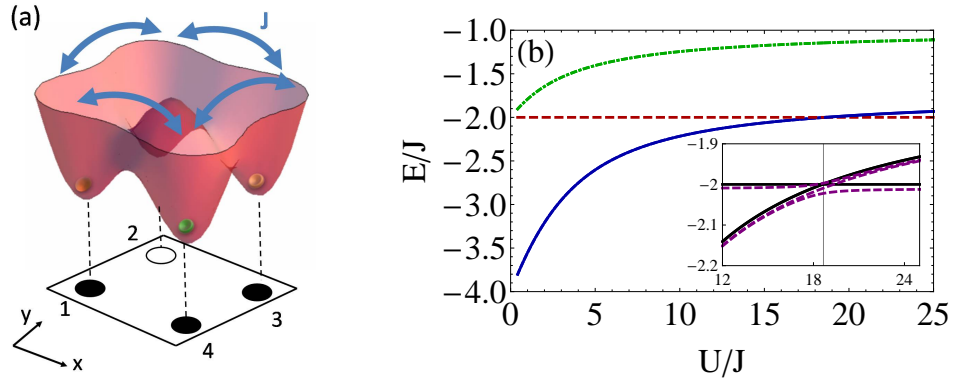


Figure 1. (a) Schematic representation of a plaquette. (b) Low energy spectrum of three fermions. Solid lines and dash-dotted are $S = 1/2$ while dashed curve corresponds to $S = 3/2$. Inset: Zoom in of the spectrum at the Nagaoka crossing. Solid lines are the spectrum for zero gradient field while dashed lines are the spectrum at finite gradient field.

The energy levels of a plaquette loaded with three fermions can be classified according to the total spin S and the symmetries of the wave function. It is known (e.g., Ref. [8]) that for $U < U_t \approx 18.6J$ the ground state is a degenerate doublet $S = 1/2$ state with $\tau = p_x \pm ip_y$ symmetry (the wave function changes phase by $\pm\pi/2$ upon $\pi/2$ rotation). For $U > U_t \approx 18.6J$, the ground state becomes a ferromagnetic $S = 3/2$ state, in agreement with the Nagaoka theorem (Fig. 1(b)). We denote these eigenstates as $|S = 1/2, S_z, \tau = \pm\rangle$ and $|S = 3/2, S_z\rangle$ with $S_z = -S, \dots, S$ and recall that the energies are independent of the S_z value. The onset of Nagaoka ferromagnetism can be understood as competition between the kinetic energy and superexchange interactions. In the $U \rightarrow \infty$ limit, double occupancies are energetically suppressed, and the low-energy

\ddagger Since a triangular lattice is not a bipartite lattice, Nagaoka theorem only holds for $J < 0$.

states are singly occupied with an energy spectrum given by $E = \pm 2J, \pm\sqrt{3}J, \pm J, 0$. The relevant low-lying eigenstates are the ones with $E^{S=3/2} = -2J$ and $E^{S=1/2} = -\sqrt{3}J$. As U become finite, while the fully polarized states remain eigenstates for any U and their energy is unaffected by interactions, the $|S = 1/2, S_z, \pm\rangle$ states acquire some admixture of double occupancies, which tend to lower their energy. The energy shift in the $S = 1/2$ states can be calculated by using second order perturbation theory, yielding $E^{S=1/2} = -\sqrt{3}J - \frac{5J^2}{U}$. The Nagaoka crossing occurs at the U_t/J value when the two energies become equal, $U_t = 5/(2 - \sqrt{3})J \sim 18.66J$, in very good agreement with the exact diagonalization.

An array of plaquettes can be created by superimposing two orthogonal optical superlattices formed by two independent sinusoidal potentials that differ in periodicity by a factor of two, i.e., $V(x) = V_s/2 \cos(4\pi x/\lambda_s) - V_l/8 \cos(2\pi x/\lambda_s)$, where V_l is the long lattice depth, V_s is the short lattice depth, and λ_s is the short lattice wavelength. By controlling the lattice intensities, it is possible to tune the intra- and interplaquette tunneling and, in particular, to make the plaquettes independent. Here the axial optical lattice is assumed to be deep enough to freeze any axial dynamics. To load the plaquettes with three atoms, one can start by preparing a Mott insulator with filling factor three in a 3D lattice and then slowly split the wells along x and y . Since only two fermions with opposite spin can occupy the lowest vibrational level, loading three fermions per site requires populating the first excited vibrational state before splitting the wells. This loading procedure creates plaquettes with $S = 1/2$.

Since S and S_z are conserved quantum numbers in clean cold atom set-ups, to probe the Nagaoka transition we require the presence of a weak magnetic-field gradient. We choose for this case a field pointing along z with a constant gradient along the x direction $\mathbf{B}(x) = \frac{\delta E_B}{\mu_B g} \frac{2x}{\lambda_s} \hat{\mathbf{z}}$, where μ_B is the Bohr magneton g is the gyromagnetic factor. The magnetic-field gradient couples the $|3/2\rangle$ state with some linear combination of $|1/2, 1/2, \pm\rangle$ which we denote as $|1/2, 1/2, 1\rangle$, through a Hamiltonian matrix element $H_{3/2,1/2} = -2/3(1 + \sqrt{3})\delta E_B$ and leaves another linear combination of $|1/2, 1/2, \pm\rangle$, which we denote as $|1/2, 1/2, 2\rangle$, uncoupled. It consequently transforms the crossing at U_t into an avoided crossing [see inset of Fig. 1 (b)] which can be used to adiabatically transform the $|1/2, 1/2, 1\rangle$, ground state for $U < U_t$, into $|3/2\rangle$ as U is slowly increased. U can be tuned by a Feshbach resonance in the presence of an external magnetic field.

The variation of $\langle S \rangle$ in the ground state below and above the Nagaoka point can be inferred from a band mapping analysis [12] after collapsing the plaquettes into single wells: The states with $S = 3/2$ and $S = 1/2$ will occupy three and two bands respectively when a plaquette is transformed into a single site. Since the state $|1/2, 1/2, 2\rangle$ remains decoupled, one can improve the band mapping signal by adiabatically turning on the magnetic field gradient at the same time the plaquettes are prepared. In this way the initial plaquette configuration will be almost in a pure $|1/2, 1/2, 1\rangle$ state and we will be able to fully transform the state into the $|3/2\rangle$ at $U > U_t$.

The energy difference between the $|3/2\rangle$ and $|1/2, 1/2, \pm\rangle$ states can also be probed dynamically. After preparing the state $|\psi(0)\rangle = \cos\alpha|3/2, 1/2\rangle + \sin\alpha|1/2, 1/2, 1\rangle$

one can suddenly turn off the magnetic-field gradient. By measuring the Neel order parameter or spin imbalance along the x direction [$N_S(t) = 1/2(\sum_{r=1,2} n_{\uparrow r} - n_{\downarrow r} - \sum_{r=3,4} n_{\uparrow r} - n_{\downarrow r})$] as a function of time, one can track the Nagaoka point by the oscillation period of $\langle N_S(t) \rangle \propto \cos[(E^{S=3/2} - E^{S=1/2})t/\hbar]$. As U/J approaches U_t/J , the period will become very long, indicating that the character of ground state has changed. This simple treatment ignores the admixture of states with double occupied sites in the $|1/2, 1/2, 1\rangle$ state. When included, the excitations introduce fast but small oscillations of frequency J . Comparisons between the exact and analytic solutions are shown in Fig. 2. The spin imbalance $N_S(t)$ can be experimentally probed by first splitting the plaquettes into two double wells and then following the same experimental methods used for measuring superexchange interactions [13] that rely on band-mapping techniques and a Stern-Gerlach filtering.

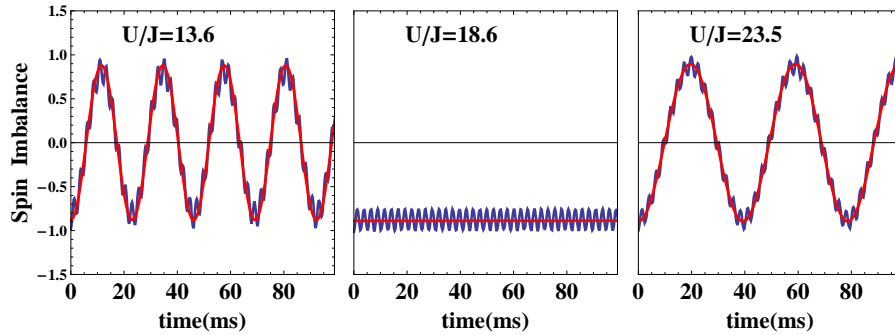


Figure 2. Normalized spin population imbalance. At the Nagaoka crossing, the envelope frequency becomes very long, indicating zero-energy splitting between the $|3/2\rangle$ and $|1/2\rangle$ levels.

The constant magnetic field needed for tuning a Feshbach resonance does not affect the dynamics since the relative energy spacing of the various levels within a plaquette is insensitive to such magnetic fields. The big advantage of this probing method is that it does not require fixing the same magnetization for the various plaquettes. Consequently, we can relax the temperature constraint for preparing the Mott insulator used for the initial loading. The insensitivity of this probing method to the initial magnetization can be understood by the fact that the dynamic taking place in a plaquette initially loaded with $S_z = -1/2$ is identical to that described for the $S_z = 1/2$ case. Furthermore, preparation of plaquettes with $S_z = \pm 3/2$ is energetically suppressed due to the large vibrational energy spacing. It should be stressed that finite temperature effects only determines the fidelity of the initial preparation of a Mott insulator. Once the Mott insulator is achieved, the observation of ferromagnetism depends on the efficiency of implementing the adiabatic manipulation discussed above.

3. Engineering long-range ferromagnetic correlations.

We now study the more general case in which one allows a weak interplaquette tunneling, J' , by lowering the long lattice depth along both the x and y directions (or along only x). This procedure generates a 2D (1D) array of plaquettes. In the Nagaoka regime ($U/J > 18.6$) to zero order in J' , the many-body ground state has a degeneracy of 4^N (N is the number of plaquettes) and is spanned by states of the form $|\Phi\rangle_{S_{z1}, \dots, S_{zN}} = \prod_i |S = 3/2, S_{zi}\rangle$. A finite J' breaks the degeneracy between the states, but as long as $J' \ll J$, the occupation of states with $S_i < 3/2$ is energetically suppressed. These states can only be populated “virtually,” leading to an effective Heisenberg interaction between the various effective $S = 3/2$ states at each plaquette [8], i.e.,

$$H_{eff} = G \sum_{\langle i,j \rangle} \vec{\hat{S}}_i \cdot \vec{\hat{S}}_j. \quad (2)$$

Here, $\vec{\hat{S}}_i = (\hat{S}_{xi}, \hat{S}_{yi}, \hat{S}_{zi})$ are spin 3/2 operators acting on the pseudospin states $|S = 3/2, S_{zi}\rangle$, and we have set $\hbar = 1$. The interaction coefficient can be written as $G = gJ'^2/J$, where $g > 0$ is an antiferromagnetic-coupling constant that slowly varies as a function of J/U . Equation (2) explicitly shows the fragility of Nagaoka ferromagnetism, since a weak coupling among the plaquettes leads to a many-body ground state with antiferromagnetic correlations.

To overcome this limitation, we consider a different initial configuration. Starting with four atoms per plaquette in the lowest orbital, we excite one of the atoms to a nondegenerate vibrational level [see Fig. 3]. This system is described by a two-band Hubbard Hamiltonian of the form

$$\begin{aligned} \hat{H} = & - \sum_{\langle r,r' \rangle, \sigma, n} J_n \hat{c}_{rn\sigma}^\dagger \hat{c}_{r'n\sigma} + \sum_{rn} U_{n,n} \hat{n}_{rn\uparrow} \hat{n}_{rn\downarrow} + V \sum_r \hat{n}_{r1} \hat{n}_{r2} \\ & - J_{ex} \sum_{r\sigma\sigma'} \hat{c}_{1r\sigma}^\dagger \hat{c}_{1r\sigma'} \hat{c}_{2r\sigma'}^\dagger \hat{c}_{2r\sigma} \end{aligned} \quad (3)$$

which is characterized by on-site interactions between particles in the ground ($U_{11} \equiv U$) and excited ($U_{22} \equiv U_e$) bands, tunneling in the lower ($J_1 \equiv J$) and upper ($J_2 \equiv J_e$) bands, and direct (V) and exchange (J_{ex}) interactions between the two bands. In the present implementation, $V = J_{ex}$. In Eq. (3), we have neglected terms that transfer atoms between bands, since they are energetically suppressed. The energy splitting between them has been omitted in our rotating frame.

A single plaquette with three atoms in the lowest band and the fourth in the second band exhibits a crossing between an $S=1$ and an $S=2$ state (ferromagnetic state) at a value of \tilde{U} that is smaller than U_t . Figure 4(a) shows the low energy behavior of this system. For the parameters used in Fig. 4(a), the crossing occurs at $\tilde{U} \approx 6J$. In general, \tilde{U} depends on J , J_e , U , and J_{ex} . Figure 4(b) analyzes the existence of a ferromagnetic ground state as a function of U/J and $\alpha_J = J_e/J$. For this analysis, we assume that the interaction terms are proportional, i.e., $J_{ex} = \alpha_{J_{ex}} U$. Different shaded regions display

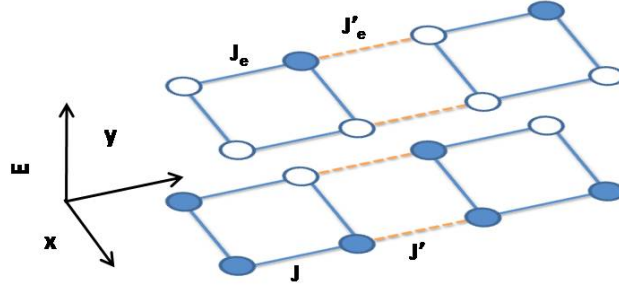


Figure 3. Schematic representation of two coupled double-band plaquettes. Solid circles represent occupied orbitals.

the ferromagnetic regions for different $\alpha_{J_{ex}}$, and the dashed curves their corresponding critical values \tilde{U} . As both α_J and α_{ex} increase, the \tilde{U} values decrease, extending the ferromagnetic region. This behavior is consistent with our physical picture that both double exchange processes and the Hund's rule coupling stabilize ferromagnetism.

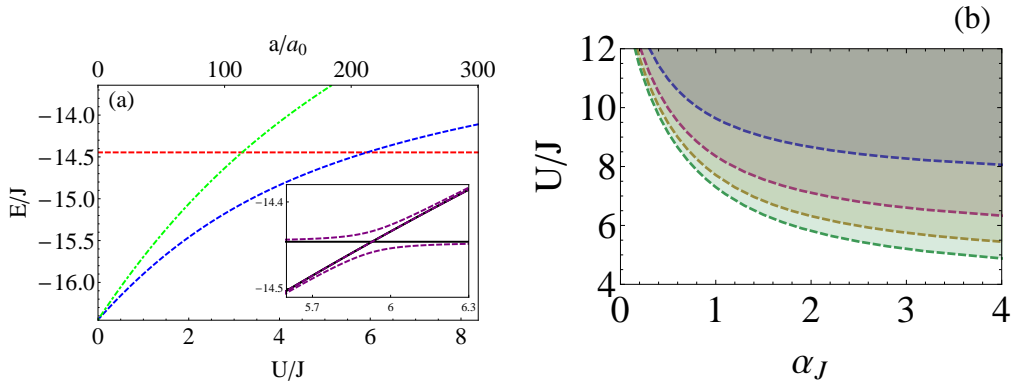


Figure 4. (a) Energies of a plaquette as a function of U/J and the scattering length in Bohr radii a_0 . The parameters that characterize the Hamiltonian [Eq. (3)] are obtained for a superlattice constructed with a short-wavelength laser of $\lambda_s = 765$ nm that characterizes the short-lattice recoil energy $E_r = \hbar^2/(2m\lambda_s^2)$. The energies of the figure corresponds to $V_l = 20 E_r$ and $V_s = 7.5 E_r$. Inset: Zoom in of the spectrum at the ferromagnetic crossing. Solid lines are the spectrum for zero gradient field while dashed lines are the spectrum at finite gradient field. (b) Ferromagnetism in a two-band plaquette. Shaded areas correspond to a ferromagnetic ground state. Dashed curves correspond (from top to bottom) to $\alpha_{J_{ex}} = 0.2, 0.4, 0.6$, and 0.8 .

The mobile atoms in the excited band are also expected to stabilize, via double-exchange processes, the ferromagnetic phase when a weak tunneling between plaquettes (J' and J'_e) is allowed. The stabilization mechanism relies on the preservation of the spin when an atom hops, and on the energy penalty of $2J_{ex}$ when ground and excited atoms form a singlet instead of a triplet at a given site. Only when the spins of adjacent plaquettes are fully aligned, the mobile atoms are free to hop. We confirm the

stabilization of the ferromagnetic correlations by studying the weakly coupled regime, which can be described again by an effective Heisenberg Hamiltonian as in Eq. (2), but now between the $S = 2$ states at each plaquette.

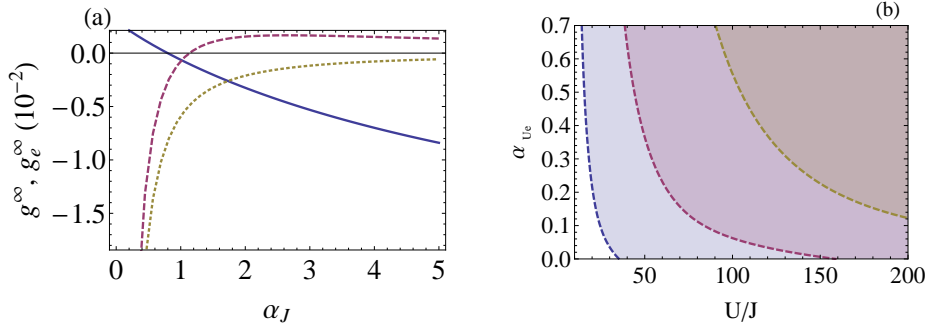


Figure 5. (a) Asymptotic coefficients g^∞ and g_e^∞ as functions of α_J . The solid curve corresponds to g , and the dotted curve corresponds to g_e . The dashed curve corresponds to g_e when $\alpha_{U_e} = 0$. (b) Phase diagram for $J' = 0$. The shaded regions correspond to the ferromagnetic regime for different α_J values. From left to right, $\alpha_J = 0.5$, $\alpha_J = 1.1$, $\alpha_J = 2$.

The coupling coefficient G can be obtained by considering virtual processes in which one atom from the ground (excited) band hops from one plaquette to the other and returns to the original configuration. In practice, we extract G from the analysis of the low-energy spectrum of two weakly coupled plaquettes [see Fig. 3]. G depends in a nontrivial way on the interaction and kinetic energy parameters and it is given by $G = gJ'^2/J + g_eJ_e'^2/J_e$ for $J', J'_e \ll J, J_e$. Here g and g_e are proportional to G when the interplaquette tunneling is allowed only in the ground or excited band, respectively. Both depend on J , J_e , U , and J_{ex} ; and g_e also depends on U_e . In the effective model, the existence of ferromagnetism can be directly deduced from the sign of G . To further understand the robustness of the ferromagnetic phase, we consider the general case for which all the interaction terms are proportional to each other, $U_e = \alpha_{U_e}U$, $V = J_{ex} = \alpha_{J_{ex}}U$, and the kinetic terms are related as $J_e = \alpha_JJ$. For large interaction values ($U \rightarrow \infty$), the coefficients g and g_e approach to their asymptotic values g^∞ and g_e^∞ that only depend on α_J (independent of $\alpha_{J_{ex}}$ and α_{U_e} so long as $\alpha_{J_{ex}} > 0$ and $\alpha_{U_e} > 0$). Figure 5 (a) shows that both g^∞ and g_e^∞ become negative for a large parameter regime, confirming the robustness of the ferromagnetic phase. If $U_e = 0$ [dashed curve in Fig. 5 (a)], g_e^∞ becomes positive for an important region of α_J values. This finding is consistent with Ref. [14] where it is pointed out that a nonzero interaction between atoms in the excited band ($U_e > 0$) can be crucial for the transition to a ferromagnetic ground state.

Figure 5 (b) shows the phase diagram as a function of α_{U_e} and U/J for three different $\alpha_J = 0.5, 1.1, 2$ values, with the assumption that $J' = 0$. For this study, we set $\alpha_{J_{ex}} = 0.4$, which is a typical value for optical superlattices. In general, we observe that as $\alpha_{J_{ex}}$ increases, ferromagnetism becomes more favorable. The transition to a

ferromagnetic ground state depends strongly on α_J and, for the $J' = 0$ case, low values of α_J enhance ferromagnetism. For $J'_e = 0$, the phase diagram is independent of α_{U_e} , and higher mobility of the excited atoms, large α_J , favors ferromagnetic correlations. For example, for $\alpha_J = 2$ the critical value U_c is $\approx 147J$. It increases to $U_c \approx 488J$ for $\alpha_J = 1.1$, and for $\alpha_J = 0.5$, no ferromagnetic phase is observed.

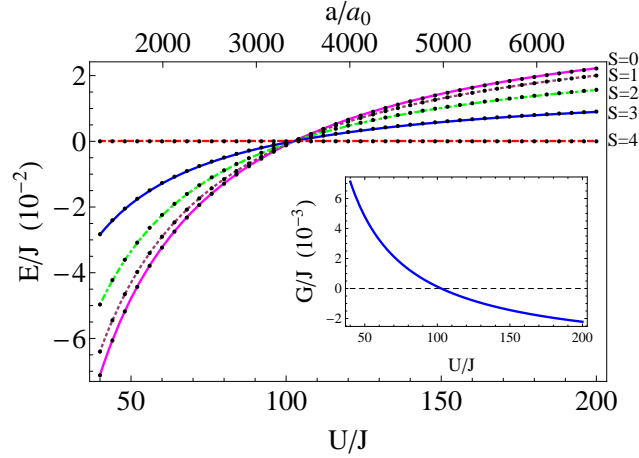


Figure 6. Lowest energies as a function of U/J and the scattering length of two weakly coupled plaquettes ($V_l = 4E_r$ and $V_s = 5.5E_r$) with six particles in the lowest band and two in the excited band and a total $S_z = 0$. Circles correspond to exact numerical calculations, and lines correspond to the effective Hamiltonian [Eq. (2)] description. Top grid: scattering length values in Bohr radii for ^6Li parameters. Inset: The G coefficient as a function of U/J for a plaquette with $V_l = 4E_r$ and $V_s = 5.5E_r$ (dashed curve). For this case, the tunneling is $J \approx 0.085E_r$. The transition occurs at $U/J \approx 100$.

However, in realistic experimental setups it is not possible to explore the complete parameter space. For standard superlattice geometries, in which only the ratio V_l/V_s controls the relation between the different tunneling parameters, we find that a favorable ferromagnetic scenario takes place in the regime when $J = J_e$ and $J' = J'_e$. We can achieve this scenario by loading the atoms in the lowest vibrational state of a 2D plaquette array (tight confinement along z) creating a 2D lattice in the $x - y$ direction and then exciting one atom per plaquette to the first vibrational orbital along the z direction. The atoms are initially all in the ground-state orbital $\Phi_g(\mathbf{r}) = \phi_0(x)\phi_0(y)\tilde{\phi}_0(z)$, and one of the atoms in each plaquette is excited to the $\Phi_e(\mathbf{r}) = \phi_0(x)\phi_0(y)\tilde{\phi}_1(z)$ vibrational state. The tunneling along the x and y directions is independent of the z -orbital ($\tilde{\phi}_0(z)$ or $\tilde{\phi}_1(z)$) and, therefore, $J = J_e$ and $J' = J'_e$. The tunneling in the z direction depends on the z -orbital but it is negligible in the 2D geometry in consideration.

Figure 6 presents this case for realistic ^6Li experimental parameters ($\alpha_{J_{ex}} = 0.5$ and $\alpha_{U_e} = 0.7$) where we observe a change in the sign of the coupling coefficient G (see inset) from positive to negative at $U/J \sim 100$, a value of interaction accessible with a Feshbach

resonance. Even though for the perturbative regime under consideration, where the effective Hamiltonian is valid, G is small (of the order of few Hz), it is measurable with state-of-the-art technology, as demonstrated in recent experiments where superexchange interactions as low as 5 Hz have been resolved [13].

For preparing and probing ferromagnetism in the isolated two-band plaquette array, we propose to start by loading atoms into a band insulator in a deep 3D lattice [15, 16]. By applying a double-well superlattice along the z -direction and manipulating the double-well bias, one can excite one of the four atoms in each double well to the first vibrational state via interaction blockade [17]. Then, by slowly merging the double wells along the z -direction and splitting them along the $x - y$ directions, one can load the desired plaquette configuration with three atoms in the lowest and the fourth in the first-excited vibrational state along z . Alternatively, spatially selective two-photon Raman pulses can be applied to excite one atom in each plaquette to the desired vibrational state [18, 19, 20]. This procedure will lead to plaquettes with $S = 0$. The state $S = 0$ can be adiabatically converted into $S = 1$ by applying a nonlinear magnetic field gradient§ along z and tuning the interactions from $U < 0$ to $U > 0$. The transition between $S = 1$ and $S = 2$ states in a single two-band plaquette can be probed using the same experimental techniques proposed for the single band plaquette. A magnetic field gradient couples the $S = 1$ and $S = 2$ states [see inset of Fig. 4(a)] and this coupling can be used to probe the transition with spin-imbalance measurements or band mapping techniques.

Interaction induced ferromagnetism in a few coupled plaquette array could also be observed by varying U/J in the presence of a magnetic field gradient. Since our initially prepared state is a band insulator with $S = 0$ the magnetic field gradient has to be large enough to couple $S = 0$ with $S = S_{max}$ across the transition. After this procedure is applied the ferromagnetic nature of the ground state can be inferred in the applied magnetic-field gradient by measuring the local magnetization of the system [21, 22, 23]. A linear magnetic-field gradient produces a perturbation in the effective Hamiltonian of the form $H_p = \sum_i i\delta E_p \hat{S}_{zi}/\hbar$, where δE_p is the average energy shift between consecutive plaquettes. In the ferromagnetic phase, the formation of a domain wall is expected. The domain-wall width will be determined by the dimensionless parameter $zGS/\delta E_p$, where z is the number of nearest-neighbor plaquettes, and $S = 2$. The measurement of this width can be used to extract G in the ferromagnetic regime. In the antiferromagnetic phase on the contrary, no domain wall will be formed, and the local Neel order parameter should vary smoothly. The onset of ferromagnetic correlations as the system is driven through the critical point should be signaled by a suppression in inelastic collisions, a minimum in kinetic energy, and a maximum in the size of the cloud. The latter signatures have been demonstrated to be useful smoking guns of a ferromagnetic transition in recent experiments carried on in fermionic gases without a lattice (See Ref. [21] and references therein).

§ Our calculations show that a simple linear gradient does not couple the $S = 1$ and $S = 0$ states.

4. Conclusions

In summary, we have proposed a controllable and experimentally realizable scheme to study interaction-induced ferromagnetism in ultracold atoms. Our method exploits the advantage offered by these systems to divide the full lattice into plaquettes.

We showed that a plaquette loaded with three fermionic atoms is a promising set-up to experimentally observe Nagaoka ferromagnetism for the first time. We also used the plaquettes as the fundamental building blocks to create interaction induced ferromagnetism at longer length scales. We analyzed the system of weakly coupled two-band plaquettes and demonstrated that in the limit where the interplaquette coupling can be treated perturbatively, the system maps out into an effective Heisenberg Hamiltonian with a coupling constant G which changes sign from positive to negative as interactions are increased. The change in sign is a manifestation of an antiferromagnetic to ferromagnetic transition.

In the perturbative regime, where our analysis is valid, the coupling parameter G is small. Consequently, it will be experimentally challenging to adiabatically reach the ferromagnetic ground state for large number of coupled plaquettes by increasing interactions. In this situation, the required temperature would be smaller than $G \sim 10^{-2}J$. Nevertheless, exact diagonalization in a two-plaquette array confirmed the persistence of itinerant ferromagnetism beyond the weakly coupling regime. Actually, we found excellent agreement between our perturbative Hamiltonian and the many-body spectrum even at values of J'/J as high as $1/4$, as shown in the low energy spectrum presented in Fig. 6. Our two-plaquette results seem to be consistent with variational Monte Carlo [24] and dynamical mean-field [25] predictions that have found ferromagnetic phases in the two-band generic square-lattice Hubbard model. The actual stability of the ferromagnetic phase in larger plaquette arrays and stronger interplaquette couplings will need however to be resolved ultimately by experiments.

Acknowledgments

This work was supported by NSF, ITAMP, CUA and DARPA.

References

- [1] D. R. Penn, Phys. Rev. **142**, 350 (1966).
- [2] E. Stoner, Proc. R. Soc. London **165**, 372 (1938).
- [3] P. Fazekas, B. Menge, and E. Müller-Hartmann, Z. Phys. B **78**, 69 (1990). A. N. Tahvildar-Zadeh, J. K. Freericks, and M. Jarrell, Phys. Rev. B **55**, 942 (1997).
- [4] Some examples of ferromagnetism in Hubbard models with complex lattice geometries have also been predicted: H. Tasaki, Phys. Rev. Lett. **75**, 4678 (1995), S. Zhang, H. Hung and C. Wu, arXiv:0805.3031, .
- [5] Y. Nagaoka, Phys. Rev. **147**, 392 (1966).
- [6] M. Takahashi, J. Phys. Soc. Japan **51**, 3475 (1982). Y. Fang *et al.*, Phys. Rev. B **40**, 7406 (1989); B. Doucot and X. G. Wen, Phys. Rev. B **40**, 2719 (1989).

- [7] E. Nielsen and R. N. Bhatt, Phys. Rev. B **76**, 161202(R) (2007).
- [8] H. Yao, W. F. Tsai, and S. A. Kivelson, Phys. Rev. B **76**, 161104 (2007).
- [9] A. Hewson, *The Kondo Problem to Heavy Fermions* (Cambridge University Press, Cambridge, 1993). H. Tsunetsugu, M. Sigrist, and K. Ueda, Rev. Mod. Phys **69**, 809 (1997); M. Gulacsi, Phil. Mag. **86**, 1907 (2006).
- [10] C. Zener, Phys. Rev. **81**, 440 (1951).
- [11] H. Tasaki, Progr. Theor. Phys. **99**, 489 (1998).
- [12] M. Greiner, I. Bloch, O. Mandel, T. W. Hansch, and T. Esslinger, Phys. Rev. Lett. **87**, 160405 (2001).
- [13] S. Trotzky, P. Cheinet, S. Fölling, M. Feld, U. Schnorrberger, A. M. Rey, A. Polkovnikov, E. A. Demler, M. D. Lukin, and I. Bloch, Science **319**, 295 (2008).
- [14] P. Simon and D. Loss, Phys. Rev. Lett. **98**, 156401 (2007).
- [15] R. Jördens, N. Strohmaier, K. Günter, H. Moritz, T. Esslinger, Nature (London) **455**, 204-207 (2008)
- [16] U. Schneider, L. Hackermüller, S. Will, T. Best, I. Bloch, T. A. Costi, R. W. Helmes, D. Rasch, A. Rosch, Science **322**, 1520 (2008).
- [17] P. Cheinet, S. Trotzky, M. Feld, U. Schnorrberger, M. Moreno-Cardoner, S. Foelling, and I. Bloch, Phys. Rev. Lett. **101**, 090404 (2008).
- [18] T. Müller, S. Fölling, A. Widera, I. Bloch, Phys. Rev. Lett. **99**, 200405 (2007)
- [19] B. Paredes and I. Bloch, Phys. Rev. A **77**, 023603 (2008).
- [20] A. Gorshkov, L. Jiang, M. Greiner, P. Zoller, and M. Lukin, Phys. Rev. Lett. **100**, 093005 (2008).
- [21] G. B. Jo, Y. R. Lee, J. H. Choi, C. A. Christensen, T. H. Kim, J. H. Thywissen, D. E. Pritchard, W. Ketterle, Science **325**, 1521 (2009)
- [22] D. Weld, P. Medley, H. Miyake, D. Hucul, D. Pritchard, and W. Ketterle, Phys. Rev. Lett. **103**, 245301 (2009)
- [23] M. Babadi, D. Pekker, R. Sensarma, A. Georges, E. Demler, arXiv:0908.3483 (2009).
- [24] K. Kubo, Phys. Rev. B **79**, 020407 (2009).
- [25] K. Held and D. Vollhardt, Eur. Phys. J. B **5**, 473 (1998).